Topical Review

Nucleic acid liquids

Gabrielle R. Abraham[1,2,†], Aria Chaderjian[2,†], Anna Nguyen[3,†], Sam Wilken[1,2,†], and Omar A. Saleh[1,2,3]

[1] Materials Department, University of California, Santa Barbara CA 93106, USA
[2] Physics Department,University of California, Santa Barbara CA 93106, USA
[3] Biomolecular Science and Engineering Program, University of California, Santa Barbara CA 93106, USA
† These authors contributed equally.

E-mail: saleh@ucsb.edu

Abstract. The confluence of recent discoveries of the roles of biomolecular liquids in living systems, and modern abilities to precisely synthesize and modify nucleic acids (NAs), has led to a surge of interest in liquid phases of NAs. These phases can be formed primarily from NAs, and driven by basepairing interactions, or through the electrostatic combination (coacervation) of negatively charged nucleic acids and positively charged molecules. Generally, the use of sequence-engineered NAs provides the means to tune microsopic particle properties, and thus imbue specific, customizable behaviors into the resulting liquids. In this way, researchers have used NA liquids to tackle fundamental problems in the physics of finite valence soft materials, and to create liquids with novel, structured and/or multi-functional properties. Here, we review this growing field, discussing the theoretical background of NA liquid phase separation, quantitative understanding of liquid material properties, and the broad and growing array of demonstrations of the potential functions of these materials. We close with a few comments discussing remaining open questions and challenges in the field.

Submitted to: *Rep. Prog. Phys.*

1. Introduction

Generally, mixtures of large molecules in solvent can exhibit equilibrium separation into distinct regions (phases), that are, respectively, dilute and dense in the macromolecule. The ubiquity of this behavior arises from: 1) The presence of chemical differences between the solvent and the subunits of the macromolecule (e.g. in atomic composition, polarity, bonding potential, etc.), which create an effective repulsion between the solvent and the macromolecule under certain conditions; and 2) the small entropy of mixing that results from the large size of the macromolecule, which limits the stability of the fully dispersed state. It is further relatively common for the dense macromolecular phase to display liquid-like properties over a broad range of conditions, as the dynamic and disordered nature of a liquid permits the macromolecules to retain internal conformational entropy that would typically be lost in a crystalline solid. Thus, a primary area of physical study is on the features of *liquid-liquid phase separation* (LLPS) of a solution into regions dense and dilute in macromolecules, with both phases behaving as liquids.

Macromolecules are prevalent in biological matter, including nucleic acids, proteins, and polysaccharides, and indeed, it has long been known that aqueous biomolecular solutions can exhibit LLPS [1]. There has been immense recent interest in biomolecular LLPS, sparked by suggestions that it is relevant for the formation of biologically-active condensed structures, including, for example, dense adhesive liquids that are secreted by certain organisms [2]; "membraneless organelles" that provide biochemical functionality and compartmentalization to the interior of living cells [3, 4]; and protocells, which have been postulated to have served as rudimentary compartments enabling the emergence of evolution by natural selection in the origins of life [5, 6]. Further interest has arisen due to the potential technological applications of condensed biomolecular phases as drug or gene delivery vehicles, biochemical reactors, or as sensors [7, 8, 9].

Here, we discuss physical aspects of LLPS in systems where nucleic acids (NAs), such as DNA or RNA, are major components of the solution. The study of such NA liquids is a burgeoning field, due in large part to the ability to exploit methods of NA nanotechnology to control key physical parameters of the constituent NA particles. NA nanotechnology is itself an emerging field [10] which exploits the ease of modern sequence-specific synthesis methods [11] to create custom-designed, nanoscale, self-assembled particles. Sequence design permits exploration of the relation between microscopic and macroscopic behaviors of an LLPS system through the control of particle shape, size, flexibility, and binding interactions. Further, the formation of dense NA phases poses intriguing electrostatic considerations, due to the large bare charge of an NA (1 e^- per base in the near-neutral pH conditions that are physiologically relevant); thus formation of dense NA phases requires reduction of inter-NA electrostatic repulsion through the use of salts and/or positively charged polymers. Given certain design parameters and electrostatic conditions, NA liquids have been shown to have material properties similar to those of biological liquids, making them insightful synthetic analogs.

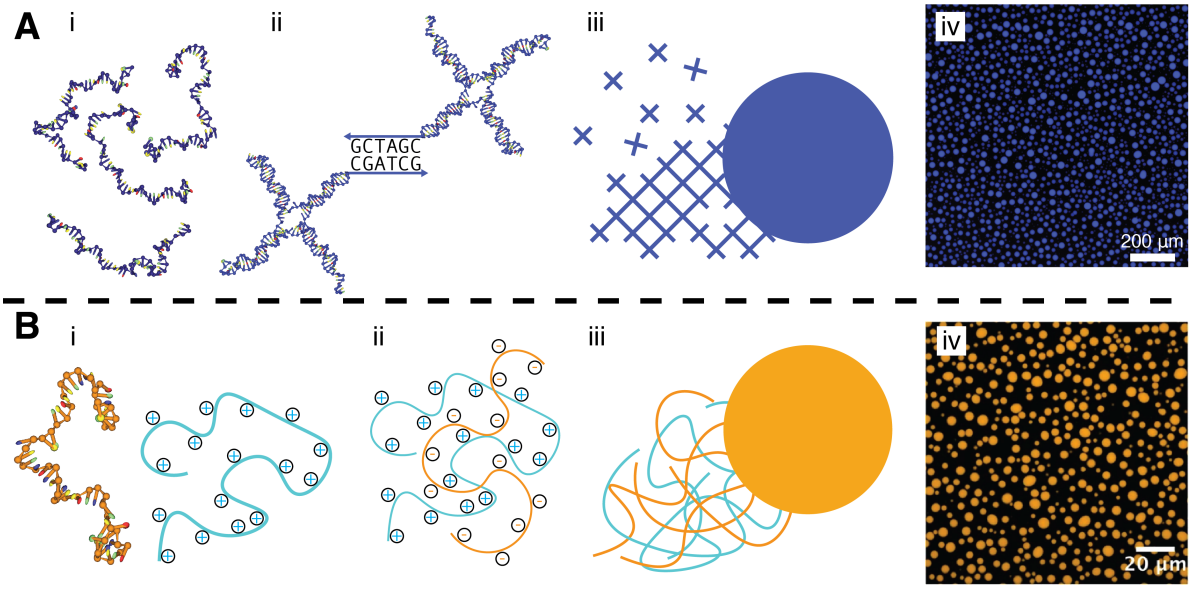

Figure 1. Two mechanisms of nucleic acid liquid-liquid phase separation. (A) (i) Single-stranded DNA oligomers are designed such that they self-assemble into junction-shaped particles ('NAJs'). (ii) These particles then condense through palindromic, sticky-end binding (i.e. hybridization of complementary single-stranded DNA regions), forming (iii) dense, disordered and dynamic meshes with liquid-like properties. (iv) Epifluorescent image of droplets composed of NAJs, adapted with permission from [13]. (B) (i) Electrostatic coacervates can be formed from negatively-charged, single-stranded NAs and positively-charge polymers. (ii) In low-salt conditions, oppositely-charged flexible polymers condense and entangle to form liquids (iii). (iv) Confocal fluorescence image of droplets composed of negatively-charged polyuracil RNA and positively-charged arginine-rich polypeptides, reprinted with permission from [14], excerpted from a larger figure.

Finally, by taking advantage of the broad array of enzymes that act on nucleic acids, NA liquids can act as models of biologically-relevant active, non-equilibrium matter.

Here, we discuss the physical principles underlying the NA phase separation process, and explore how various authors have exploited those principles to create a range of NA liquids. While most of this review focuses on dense phases formed due to base-pairing interactions between branched NA structures (Fig. 1A), we also discuss NA-based "coacervates," which are dense liquid phases induced by electrostatic interactions (Fig. 1B). Throughout, we include both historical context and theoretical perspectives, the latter inspired by both colloidal and polymeric analyses, as well as experimental results on phase and material behavior. Lastly, we review recent compelling demonstrations of the structures and functionalities of NA liquids, and conclude by discussing notable future challenges in the field. For an alternate perspective, we point the reader to a recent insightful review of phase-separated DNA liquid droplets [12].

2. Development of NA junction liquids

NA particles containing branched junctions are a common motif in the study of biomolecular LLPS. Indeed, there are naturally-occurring RNA sequences that fold into branched particles, and that are known to associate and undergo phase separation *in vitro*; there is also evidence that interactions between such branched RNAs contribute to *in vivo* LLPS [15]. In synthetic (non-biological) contexts, NA junctions are typically composed of several NA oligomers whose sequence causes them to self-assemble, via Watson-Crick base-pairing, into a branched structure consisting of double-stranded "arms", each decorated with a single-stranded "sticky-end" [16] (Fig. 1A). These structures resemble Holliday junctions, transient branched structures that occur in biology during genetic recombination [17]. A key difference is that Holliday junctions are typically 'homologous', with matched sequences between pairs of NA arms, which enables migration of the branch point[18]. In contrast, most synthetic NA junctions are 'heterologous', lacking such sequence symmetry, and thus have a fixed branch point. Synthetic NA junctions have been given various names in the literature, including "X-DNA" [19] and "nanostars" [16]. Here, we call them nucleic acid junctions (NAJs).

Creating materials out of NAJs was initially proposed by Seeman, who was inspired by M. C. Escher's artwork *Depth* to create DNA particles that would self-assemble into 3-dimensional ordered lattices [20]. Seeman and colleagues created 4-armed NAJs, but concluded that such designs were too flexible to create the crystalline DNA structures that were their primary aim [21, 22]. This internal flexibility, when combined with strong (covalent) inter-particle attractions, promotes formation of static disordered networks (i.e. NAJ hydrogels), a material pioneered by Luo and colleagues [19] whose behavior and potential applications have since been investigated by a variety of authors [23, 24].

Liquids composed of NAJs were first explicitly demonstrated by Biffi *et al.* in 2013, in a study of 3- and 4-armed NAJs [16]. Their investigation was motivated by a desire to mimic, at larger length scales, the posited hidden LLPS behavior of supercooled water [25], whose unique features have been attributed to water's tetrahedrally coordinated 'network liquid' structure [26, 27, 28]. Biffi *et al.* first quantified the basic upper-critical-temperature phase behavior of NAJ liquids, and its dependence on valence, along with carrying out initial studies on dynamics [16]; these topics are discussed further below.

2.1. NAJ liquid phase behavior

Modeling of long single- or double-stranded NAs is typically done from a polymeric perspective, due to their linear nature. However, the compact and branched nature of NAJs demands an alternate approach. Indeed, significant theoretical progress in predicting NAJ phase behavior has been made by approximating them as hard spheres with highly-directional attractive patches, i.e. as "patchy colloids" (Fig. 2A). For such particles, Wertheim developed a thermodynamic perturbation theory that modified a reference fluid, with spherically symmetric particle interactions, through the addition

of an anisotropic perturbing pair-potential [29]. This theory, and extensions thereof (in particular, the Statistical Associating Fluid Theory [30]), has been successful in describing phase equilibria of molecular fluids with hydrogen bonding associative interactions [31] and the assembly of patchy colloidal particles [32].

To capture the phase behavior of NAJ systems, Rovigatti *et al.* extended the Wertheim theory to incorporate the thermodynamics of DNA hybridization [33]. They gave the following form of the free energy per particle, in units of k_BT, as a function of the NAJ number density (c_{NAJ}), including terms associated with the ideal gas entropy ($Log[c_{NAJ}]-1$) and the NAJ excluded volume (Bc_{NAJ}), where B is the second virial coefficient:

$$\begin{aligned}\bar{F} &= Log(c_{NAJ}) - 1 + Bc_{NAJ} \\ &+ f\left[Log\left(\frac{-1+\sqrt{1+4\Delta f c_{NAJ}}}{2\Delta f c_{NAJ}}\right) + \frac{1}{2}\left(1 - \frac{-1+\sqrt{1+4\Delta f c_{NAJ}}}{2\Delta f c_{NAJ}}\right)\right]\end{aligned} \quad (1)$$

The final term encompasses the effect of multivalent DNA hybridization, where f is valence, or the number of sticky ends per NAJ, and Δ is related to a Boltzmann factor of the sticky-end binding free energy, ΔG: $\Delta = (1.66\ \mathrm{nm}^3)e^{-\Delta G/k_BT}$ [34]. ΔG can be calculated from the sticky-end sequence using established methods of DNA thermodynamics [35]. Equilibrium phase boundaries are calculated from Eq. 1 by the common tangent construction, such that the chemical potential ($\mu = \bar{F} + \rho\frac{\partial \bar{F}}{\partial c_{NAJ}}$) and the pressure ($P = c_{NAJ}^2\frac{\partial \bar{F}}{\partial c_{NAJ}}$) are equal in the dense and dilute phases.

The resulting coexistence phase diagram is predicted to depend strongly on the valence, f [36, 34] (Fig. 2A). Indeed, Conrad *et al.*, carried out phase diagram measurements of NAJs of various valence, finding quantitative agreement of measured T_c with the predictions of Eq. 1(Fig. 2B) [37]. For sufficiently low temperatures, all valences displayed vanishingly small dilute phase density [34, 37], indicating almost all NAJ particles accumulate in the dense phase.

In contrast to the electrostatic coacervates discussed below, NAJ concentration in the dense phase is remarkably low, with a DNA volume fraction of $\phi \approx 1\%$ for $f = 4$ NAJs with 20 basepair arms [16, 38]. Further, both prediction (Eq. 1) and experiment indicate that liquid density increases with valence [34, 37], making NAJs a physical realization of so-called "empty" liquids predicted by Bianchi *et al.* (Fig. 2) [36]. These low densities are due, first, to the small number of neighbors of each particle, as enforced by their finite valence, meaning the NAJ networks tend to be quite open [39]. Further, the rigid nature of the NAJ's double-stranded arms, whose typical length of 10 nm is much less than the DNA persistence length $\approx$ 50 nm [40], means each particle occupies only a small fraction of its pervaded volume. This indicates particle-particle excluded volume is not dominated solely by steric effects, but also includes significant contributions from electrostatic repulsion of the negatively-charged DNA [41]. Thus NAJ liquid density is tunable by adjusting the concentration of added salt, which modifies electrostatic screening [38, 42, 37]. Other works have also indicated alternate

means to tune liquid density, e.g. through NAJ arm length [43] or flexibility [42].

The Wertheim picture does not consider competition with other dense NAJ phases, such as ordered phases. This was investigated in simulations by Rovigatti *et al.*, which indicated that the thermodynamically stable low-temperature phase is, in fact, a fully bonded *liquid* network [44]. This contrasts with typical systems, where the low-temperature disordered liquid is a metastable state with respect to lower-energy crystalline configurations. The difference arises from the limited valence and the flexibility of the NAJ particles; the latter causes the NAJs to resist the formation of a regular, periodic structure in favor of maximizing the entropy of the arm orientation [44].

The relation between particle-scale NAJ design parameters and NAJ phase behavior has been investigated in a variety of works, beyond the results on valence already mentioned [34, 37]. For example, Nguyen *et al.* showed that an NAJ system that formed liquid droplets could be induced to instead form a solid, fractal-like gel simply by removing a single unpaired base between the NAJ sticky-end and arm [45]; this likely occurred because removal of that base added *two* base stacking interactions, significantly strengthening the NAJ–NAJ bond. Later, Sato *et al.* performed a careful, systematic variation of the sticky-end bond strength by varying its sequence, finding it to directly control the melting temperature of an NAJ liquid [46]. More subtle effects arise from modulating NAJ arm flexibility, which Lee *et al.* achieved by incorporating single-stranded regions in each double-stranded arm [42]; this was found to discourage phase separation by enabling self-passivation (i.e. binding between two arms from the same NAJ).

2.2. Material behaviors of NAJ liquids

The unique phase behavior of NAJ liquids is joined by interesting material behaviors. In a range of works [16, 28, 47], Sciortino *et al.* used dynamic light scattering to measure density fluctuations within the NAJ liquid, finding them to be highly sensitive to the kinetics of individual sticky-end bonds. NAJ liquids show a dramatic (Arrhenius) slowing of dynamics with bond strength (e.g. at lower temperature, or higher salt), which can be directly predicted through an activation barrier controlled by the sticky-end binding enthalpy [16, 28, 48, 38]. This eventually leads to an 'equilibrium gel' behavior when bond kinetics are slower than the observable timescales, and the system structure is representative of one member of the ensemble of liquid configurations [39].

The primary role of single-bond kinetics was also found in bulk rheology studies by Conrad *et al.* [49], who showed that NAJ liquids behave like simple Maxwell viscoelastic materials, with a well-defined elastic plateau at short timescales and Newtonian viscous behavior on long timescales. Notably, the measured NAJ liquid viscosities were more than 1000-fold larger than water [49], as also found in prior work [38]. The characteristic crossover time was found to be consistent with the kinetics of single inter-NAJ DNA bonds [49] (Fig. 3). Further, Conrad *et al.* found the modulus of the elastic plateau to greatly increase with NAJ valence [49]. This finding, and other features, was interpreted

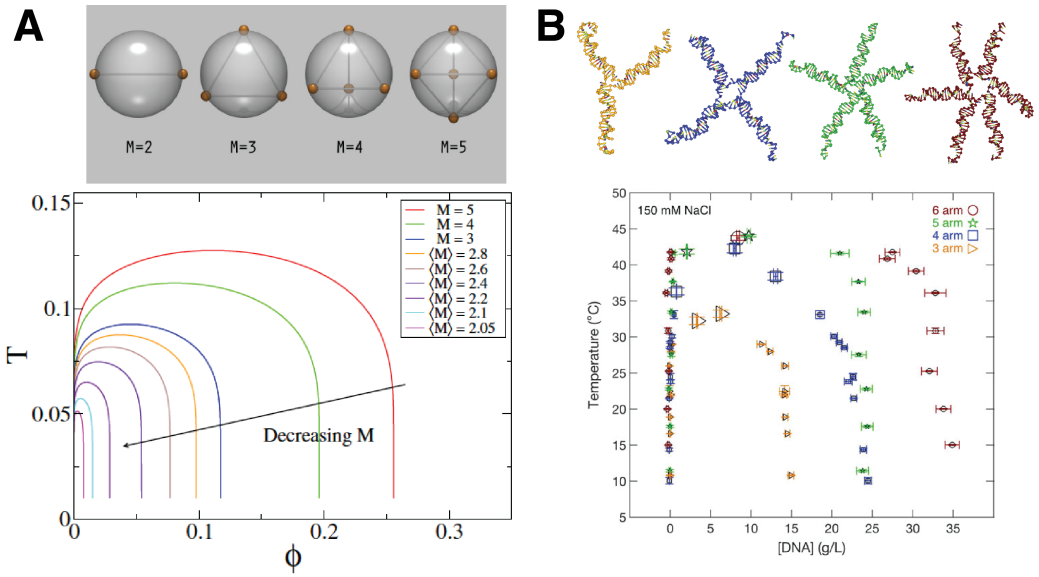

Figure 2. Phase diagrams (i.e. the binodal lines and contained coexistence regimes) as a function of valence from (A) theoretical calculations of patchy colloids (where here M is the valence, rather than f as in Eq. 1) and (B) experimental measurements of NAJs. (A) Reprinted figure with permission from [36] Copyright 2006 by the American Physical Society. (B) Reprinted from [37], with the permission of AIP Publishing.

to indicate that the mechanics of high valence ($f \geq 5$) NAJs are controlled by an isostatic point, i.e. that stiffening with valence is due to the disappearance of floppy modes within system, as caused by the constraints of the increasingly-connected network [50, 51].

The high water content of NAJ liquids implies a characteristic length scale (a mesh size) below which the liquid is easily pervaded by neutrally-interacting solutes (i.e. those with only steric interactions with the NAJs). Unlike a static gel, some nuance is needed in interpreting the meaning of a mesh size in a dynamic liquid. In analogy to the thermodynamics established for quantifying the hydrophobic free energy associated with transferring a non-polar solute into water, where the initial creation of a cavity in the water plays a large role [52], the mesh size in an NAJ liquid is likely best interpreted as the length scale beyond which it costs significant energy ($\gg k_BT$) to create a void that excludes NAJs, i.e. is filled only with solvent. Nguyen *et al.* estimated the mesh size to be $\approx$ 8 nm in an $f = 4$ NAJ liquid, using fluorescent quantification of partitioning of dextran of various sizes [53]. This length is, sensibly, similar to the length of the NAJ arm used in that study. Further, extending the thermodynamic analogy just mentioned, one is motivated to estimate the mesh size as the scale, r, at which creating a water-filled void costs k_BT in interfacial energy, i.e. $4\pi r^2\gamma \approx k_BT$, where γ is the NAJ/dilute solution interfacial tension. Using prior measurements of γ (discussed further below)[38], this estimate gives $r \approx 13$ nm, surprisingly close to the Nguyen *et al.* value. This estimate is somewhat rough, as it ignores specific molecular arrangements that are available to NAJs in surrounding voids, but the similarity with

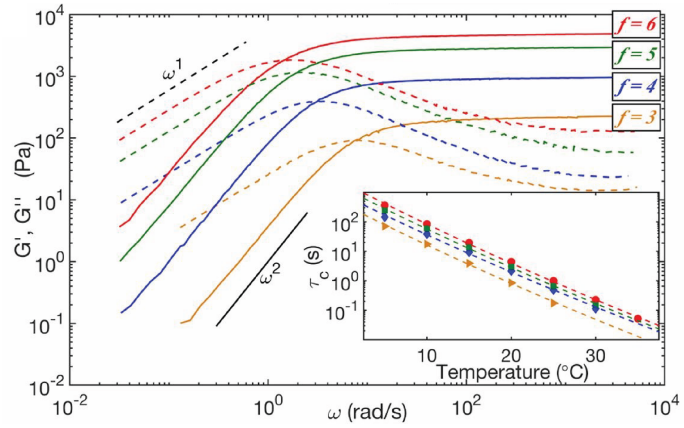

Figure 3. Frequency-dependent mechanical response of an NAJ liquid. Storage modulus G' (solid lines) and loss modulus G'' (dashed lines) vs. frequency, ω, for different valence, f. All valences behave like Maxwellian viscoelastic fluids, with low-frequency Newtonian-liquid behavior ($G'' \propto \omega$) and high-frequency elastic behavior ($G' \propto const.$) separated by a crossover timescale $\tau_c = 2\pi/\omega_c$. Inset: For a range of temperatures, τ_c exhibits Arrhenius behavior ($\tau_c \propto e^{E_a/k_BT}$), with a characteristic activation energy E_a that is the same for all f and approximately equal to the enthalpy of hybridization of a single sticky end of the given sequence [35]. Reprinted with permission from [49]

the measurement indicates it likely captures the basic physics. Further details on the microstructure of dense NAJ liquids are an open question, though certain features have been elucidated in a scattering study by Spinozzi *et al.* [41].

Much work (discussed below) has focused on droplets of NAJ liquids. Droplets present a high interfacial area (i.e. between dense and dilute NAJ phases), yet there have been relatively few quantitative studies of interfacial behavior. Jeon *et al.* inferred the interfacial tension of $f = 4$ NAJ droplets from coalesence timescales, finding values $\approx 10^{-6}$ N/m [38]). A study of $f = 3$ NAJ droplets by Sato *et al.* estimated even lower interfacial tension values [54]. These values are orders of magnitude lower than that of truly molecular systems (e.g. oil/water has $\approx 10^{-2}$ N/m), which is expected given the larger size of the particles in NAJ liquids. Less obviously, it is less than typical estimates of interfacial tension of electrostatic coacervates ($\approx 10^{-4}$ N/m [55]), though comparable to that of certain biological liquids [56]. The low surface tension indicates that NAJs at the interface exhibit an exceptionally small energy penalty, which Jeon *et al.* interpreted to mean that there is little bond-breaking at the interface, perhaps because NAJ internal flexibility allows particles at the interface to orient their arms to the interior [38]; however, direct proof of this is currently lacking.

2.3. Mesoscale dynamics of NAJ liquid formation

Liquids undergoing phase transitions can exhibit rich dynamical behavior on scales longer than a single particle. Notably, such systems typically display enhanced fluctuations in the vicinity of the critical point (i.e. near the critical temperature

and concentration). Such relaxation dynamics are expected to display critical slowing down, characteristic of the Ising universality class [57]. However, evidence of Ising scaling in NAJ dynamics was not seen in light scattering measurements near the critical temperature [16]; instead, relaxations due to single-bond DNA hybridization kinetics dominated for all experimental measurements, as discussed above. This is likely a consequence of the long lifetime of DNA bonds relative to the time necessary for free unbound NAJ particles to diffuse distances of order the correlation length [16, 58].

The dynamics of droplet assembly also play an integral role in the formation of long range structures in phase-separated systems. Wilken *et al.* imaged fields of NAJ droplets after a temperature quench (as in Fig. 1A) and found that they formed surprisingly regular, i.e. "hyperuniform", patterns on long length scales [13]. Particularly, the imaged structure displayed a power-law decay of density fluctuations characteristic of hyperuniformity, with structure factor $\psi(q \to 0) \propto q^2$. By comparing experimental measurements to simulations of the Cahn-Hilliard equation (a ubiquitous phase-field representation of spinodal decomposition), the authors argued that the hyperuniformity exhibited by NAJ droplets results from the interplay of spontaneous phase separation and droplet Brownian motion (Fig. 4). Notably, NA droplets formed by the electrostatic coacervation of polypeptides and nucleotides were found to display the same characteristic decay of density fluctuations ($\psi(q \to 0) \propto q^2$) as NAJ droplets, though the mechanisms for phase separation are completely different [13]. The observed hyperuniformity in these two orthogonal systems suggests a universal mechanism for forming hyperuniform patterns from phase-separated materials; Wilken *et al.* suggest that such materials could find applications that exploit the exotic structural and dynamical collective properties enabled by their hyperuniform structures[13].

3. NA-based electrostatic coacervates

Negatively-charged NAs can also undergo LLPS due to attractions with cations or polycations (Fig. 1B). Such electrostatically-driven LLPS, referred to as "coacervation" by Bungenberg de Jong and Kruyt, was first observed in solutions containing polysaccharides and proteins [1]. Contrary to NAJ liquids, NA coacervates are destabilized by increasing salt concentration. This arises from the different attractions that drive phase separation — for NAJs, salt-induced screening enhances sticky-end hybridization by reducing like-charge repulsion, while for NA coacervates screening weakens the opposite-charge attraction. Even though binding isn't driven by sequence-specific hybridization, researchers have still exploited NA programmability to explore the coacervate state.

3.1. Theoretical understanding of NA coacervates

The basic picture of electrostatically-driven phase separation of polymeric systems is achieved by the Voorn-Overbeek model [59]. Voorn-Overbeek is a mean-field theory

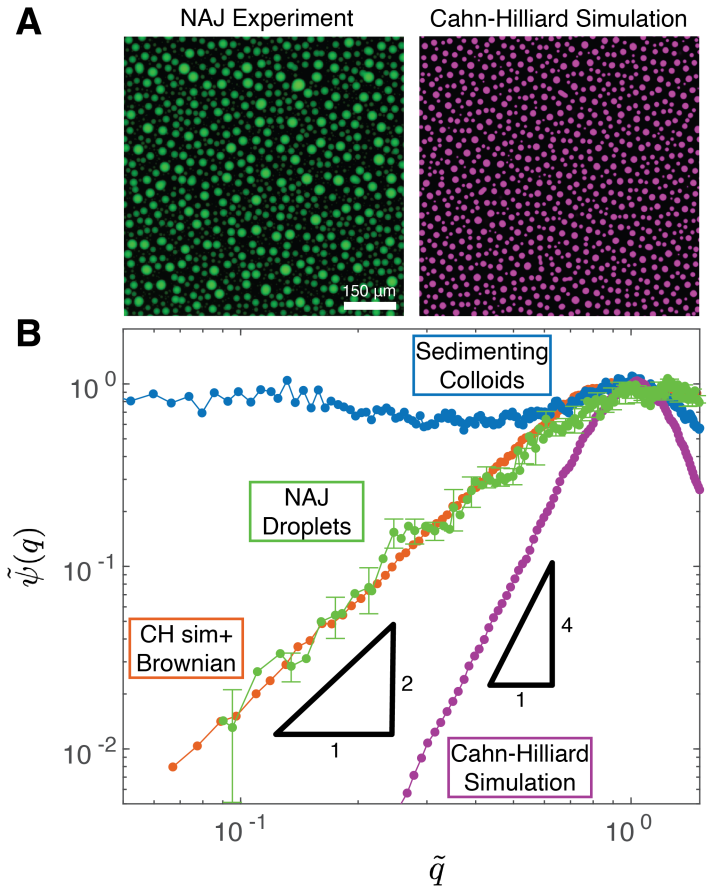

Figure 4. (A) Left: Fluorescent experimental image of the long-range pattern of NAJ droplets; Right: image of the droplet pattern formed by simulation of the Cahn-Hilliard equation. (B) The spatial auto-correlation function $\psi(q)$ of phase-separated NAJ droplets as a function of wavevector, q, shows hyperuniform scaling $\psi(q \to 0) \propto q^{\alpha}$ in the experiment (green), with exponent $\alpha = 2$, as well as in Cahn-Hilliard simulations (magenta), with $\alpha = 4$. The experimental hyperuniformity is recovered by randomly displacing the simulated droplets with a magnitude corresponding to one average droplet spacing (orange). ψ of 10-μm-diameter polystyrene colloids (blue) are random (i.e. not hyperuniform). Values of ψ are normalized for comparison: $\tilde{\psi} = \psi/\psi_{peak}$ and $\tilde{q} = q/q_{peak}$. Reprinted with permission from [13], excerpted from a larger figure.

that combines terms describing the entropic penalty of demixing (as described by Flory-Huggins theory [60]) with the Debye-Hückel theory for the free energy of a charged liquid [61]. The free energy change of demixing per lattice volume, ΔF, in units of $k_B T$, is a function of the volume fraction ϕ_i, the number of monomers N_i, and the charge density σ_i for each component i:

$$\Delta F = \sum_i \frac{\phi_i}{N_i} ln\phi_i - \alpha(\sum_i \sigma_i \phi_i)^{3/2} + \sum_i \sum_{j<i} \chi_{ij} \phi_i \phi_j. \tag{2}$$

where the Flory parameter χ describes any additional, non-electrostatic interactions, and $\alpha = \frac{2}{3}\sqrt{\pi}\,(l_B/l)^{3/2}$ is the electrostatic interaction parameter and is a function of the Bjerrum length l_B and the monomer size l.

The Voorn-Overbeek theory has provided valuable insights for understanding coacervation, and numerous studies [62, 63], including on NAs [64], have shown this model can phenomenologically capture experimental results, if various constants (such as χ and α) are treated as fitting parameters. However, the complexities of electrostatic interactions, and particularly the need to carefully consider the behavior of both salt and polymeric ions, makes it difficult to use VO theory to make accurate *a priori* predictions, which contrasts with the status of the Wertheim picture of NAJs captured in Eq. 1. Developing more accurate theories and models for coacervation remains an active area of research [65, 66].

3.2. Experimental study of NA coacervates

Simple coacervates, largely stabilized by electrostatic interactions, can be formed from a single NA that is not capable of basepairing, mixed with multivalent salt ions. Simple NA coacervates have been formed with, for example, long RNA molecules (of order kilobases) and divalent salts (e.g. Mg^{2+} or Ca^{2+}) [14] and short ssDNA sequences ($\approx$ 90 bases) with tetravalent ions (e.g. spermine) [67]. Generally, a prediction of Voorn Overbeek theory (Eq. 2) is that longer chains will be more prone to phase separation, due to their reduced entropy of mixing.

Recent works have examined the interplay between electrostatic and other interactions in NA coacervates. For example, Merindol *et al.* found conditions in which, in the presence of divalent cations, purine-rich ssDNA would coacervate, but not pyrimidine-rich ssDNA [68]; they attributed to this to the ability of purines to take part in certain specific, but non-basepairing, interactions [68]. Other authors have investigated the interplay of electrostatic coacervation with inter-NA basepairing interactions, generally finding an increase in dense-phase stability, or even gel formation, of the resulting material [67, 69, 70, 71, 72]. Such non-electrostatic contributions to coacervation can, in theory, be accounted for through the χ parameter in Eq. 2, an approach taken by Onuchic *et al.* [14].

A striking finding is that coacervates composed of short dsDNAs can form liquid crystalline (LC) phases, due to the mutual alignment of the constituent rod-like particles (Fig. 5). Early investigations discovered LC formation when mixing dsDNA and multivalent polyamines (e.g. spermine) [73, 74]. Further, several studies have observed LC behavior for dsDNA spanning only 6 to 22 basepairs [75, 76, 77], despite these short lengths being below the theoretical limit for LC condensation [75, 78]. This puzzle was recently clarified by Fraccia *et al.*, who found LC formation of short duplexes requires dsDNA with blunt ends, which allows for end-to-end base-stacking, effectively introducing a second intermolecular interaction favoring alignment [77].

Complex coacervation refers to the phase separation of mixtures of oppositely charged macromolecules (rather than a single macromolecule and an oppositely-charged microscopic ion; see Fig. 1B). The biological relevance of complex coacervation was initially explored in the 1950s and 1960s in the context of mimicking the

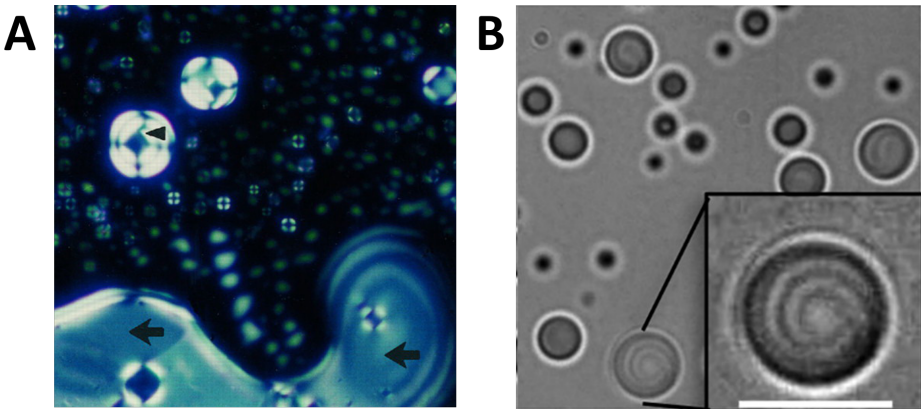

Figure 5. Cholesteric DNA Liquid Crystals (A) dsDNA complexed with spermidine, arrows indicated planar textures magnification 400x (scale bar not given). Reprinted with permission from [74], excerpted from a larger figure and cropped. (B) dsDNA complexed with PLL, scale bar 5 μm. Reprinted from [76], with permission from Elsevier.

genomic packaging of DNA with positively-charged histones [79, 80]. Contemporary investigations have shifted toward simpler model systems so as to understand the impact of fundamental NA properties, such as sequence and secondary structure, on complex coacervation. For example, ssDNA and poly-L-Lysine (PLL) form liquids over a wide range of salt concentrations, whereas dsDNA readily forms gel-like precipitates at similar salt concentrations [81, 76]. This is likely due to dsDNA's higher charge density creating stronger electrostatic interactions that disallow molecular-scale dynamics, and is thus similar to the observation discussed above regarding gel formation in NAJ liquids with strong bonds [45]. In agreement with this interpretation, Vieregg *et al.* found that replacing the negatively charged phosphates on a dsDNA backbone via methylation (thus weakening electrostatic interactions) produced liquid droplets instead of precipitates [81]. Further, in line with Voorn-Overbeek predictions discussed above, they also found that longer polymers facilitate phase separation in complex coacervates [81].

4. Structured, active, and functional nucleic acid liquids

Much recent work on NA liquids has focused on exploiting the ease of NA sequence designability to create complex meso-scale structures, to imbue the liquids with biomimetic active (driven, non-equilibrium) behaviors, or to create functional, responsive liquids. These are broad and cutting-edge areas, and in this section we aim to give a general overview of relevant activity.

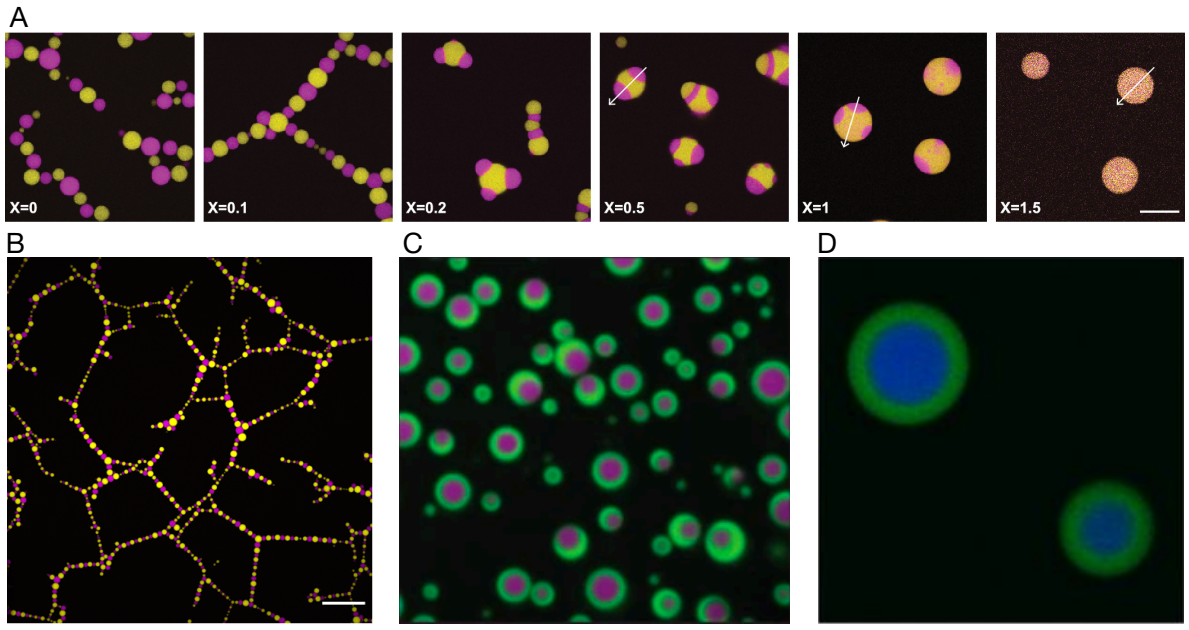

Figure 6. Fluorescent images of multiphase NA droplets. (A) In the presence of two immiscible NAJ droplet species, tuning the amount of crosslinker NAJ (X) relative to that of the other NAJs results in a variety of morphologies. Scale bar 20 μm. (B) Wide-field view of the long-range droplet morphology formed at $X = 0.1$, showing a branched network of chains of binary droplets. The chains are straightened by coalesence-induced contraction of initially tortuous, percolated, droplet aggregates. Scale bar 100 μm. Panels (A) and (B) reprinted with permission from [84]. Copyright 2020 American Chemical Society. (C) Nested droplets of polyuracil coacervates formed by adding UTP, with regions of polylysine (green) and polyarginine (purple). Droplets are of order 5 μm. Reprinted with permission from [85], excerpted from a larger figure. (D) Nested droplet structures formed from cholesterol-decorated NAJs, where the regions vary in NAJ arm length. Droplets are of order 20 μm. Reprinted with permission from [86], excerpted from a larger figure.

4.1. Multiphase droplets

The growing understanding of the cell interior as a subspace of compartments, in part driven by LLPS processes [3, 4, 82, 83], has motivated the *in vitro* creation of coexisting phase-separated domains of NA liquids. For NAJs, Jeon *et al.* and Sato *et al.* showed distinct compartments can be created using particles with orthogonal (non-binding) sticky-end sequences [84, 46]. Jeon *et al.* also showed that the compartment morphology, and even the miscibility of the two orthogonal NAJs, can be systematically tuned by varying the stoichiometry of phase-separating NAJs relative to a third "crosslinking" NAJ that contains both sticky-end sequences (Fig. 6A)[84]. A striking finding was that including the proper proportion of the crosslinking NAJ led to the formation of branched networks of binary droplet chains that spanned long distances (millimeters; Fig. 6B). This is, to our knowledge, a unique demonstration of sequence-engineered creation of specific long-range NA droplet structures.

While the existence of distinct NA liquids relies on bulk energetics (as described by

Eqs. 1 and 2), the morphology of multiphase structures depends on relative interfacial energies. Indeed, recent work has predicted the entire set of topologically-distinct morphologies in a multicomponent system from simple inequalities associated with the various interfacial tensions [87]. In the context of synthetic complex coacervates, Lu *et al.* successfully formed nested-droplet geometries, and argued that the relevant interfacial tensions can be understood through Voorn-Overbeek predictions and the charge density of the constituent polymers [88]; others have demonstrated similar structures in NA coacervate systems (Fig. 6C) [85, 89, 90, 76, 88]. The lack of detailed knowledge of the interfacial properties of NAJ liquids (discussed above) has thus far precluded similar control of nested NAJ droplet morphologies. That said, nested-droplet structures have been demonstrated in a related system of cholestrol-functionalized NAJs, by varying the length of the constituent arms [86] (Fig. 6D).

4.2. Enrichment of solutes

The biocompatibility and open structure of NA liquids allow functionalization of the droplets using a variety of solutes. For NAJ liquids, the dense phase is stabilized by sequence-specific bonds (i.e. the sticky ends), therefore solutes can be driven into the dense phase by tagging them with those same sticky ends. This has been used to partition ss- and ds-DNA [84, 53, 91], biotin-streptadivin complexes [46, 84, 92] and kinesin [93] into NAJ droplets, or even within select phases of a multi-phase system [84, 46, 91] (Fig. 7A). In the case of dsDNA, Nguyen *et al.* found a nuance in which longer solutes were excluded relative to shorter solutes with the same number of binding sites [53]. The authors quantitatively related this exclusion to the entropic penalty of confining long DNA inside the dense NAJ mesh (thus limiting transverse fluctuations) [53]. A downside of targeting the NAJ sticky ends is that, at high solute concentrations, the competition for sticky ends can destablize the NAJ liquid [91]. To avoid this, NAJs have been designed to include a toehold sequence, unique from the sticky end, that enables solute partitioning [91, 86] (Fig. 7B).

4.3. Encapsulating biochemical reactions

In biological systems, the specific role that liquid phase transitions play in regulating or enhancing biochemical reactions has been the source of much recent interest [3, 95]. Because NA liquids can locally concentrate biomolecules, they present an ideal environment to explore the impact of phase transition dynamics on biochemical reactions. Do *et al.* [91] performed strand displacement reactions (Fig. 7C), including simultaneous reactions occurring in multiple immiscible NAJ phases, and found that they were accelerated 26-fold in the NAJ liquid phase relative to the dilute phase. This acceleration is less than that expected from predictions based simply on the concentration difference in the phases, which the authors posited was due to retardation of dynamics by the high viscosity of the dense NAJ liquid[91]. It has been proposed that such strand-displacement reactions, as enabled by and coupled to NAJ liquids, could act

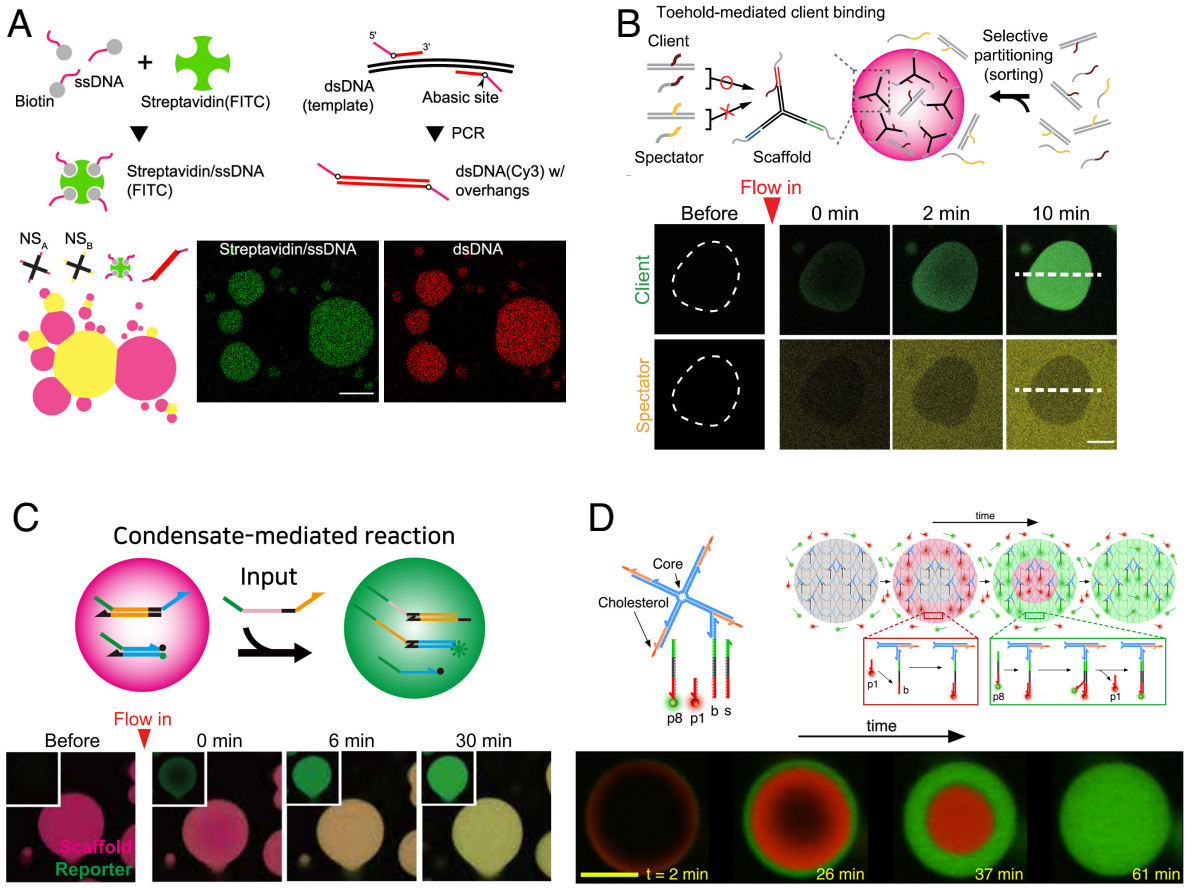

Figure 7. Schematics and fluorescent images describing solute enrichment and reactions inside NAJ droplets. (A) Streptavidin and dsDNA functionalized with A-type overhangs allow selective partitioning into the A phase and exclusion from the B phase of an NAJ liquid. Scale bar 10 μm. Reprinted with permission from [84]. Copyright 2020 American Chemical Society. (B) A toehold design allows ssDNA and dsDNA solutes with sequences complementary to the toehold to partition into NAJ droplets, whereas clients that are not complementary partition to a much lesser extent. Scale bar 20 μm. (C) Strand-displacement reactions mediated by an NAJ droplet. Droplet of order 40 μm. (B) and (C) adapted from [91]. Copyright The Authors, some rights reserved; exclusive licensee AAAS. Distributed under a CC BY-NC 4.0 license. Reprinted with permission from AAAS. Panels excerpted from larger figures. (D) Dynamic patterned structures formed by a two-step cascade of ssDNA solute invasion into cholesterol-decorated NAJ droplets. Scale bar 15 μm. Adapted with permission from [94], excerpted from a larger figure.

as reporting biosensors that can even perform simple computations, e.g. act as AND, NOT or OR gates depending on specific inputs of signal NA strands [96, 91]. Leathers *et al.* showed that strand-displacement reactions can be used to pattern NAJ droplets (Fig. 7D); separately, and impressively, this work incorporated active transcription into the droplets [94].

Studies of reaction engineering are more widespread in NA coacervates. For example, Schoenmakers *et al.* created *in vitro* biomolecular coacervates with specific

compositions of proteins and NAs capable of performing both transcription and translation [97]. Le Vay *et al.* found that, within droplets formed from coacervation of ribozymes (an RNA enzyme) and PLL, the ribozymes displayed an enhanced catalytic rate and yield [98], and further that droplets containing active ribozymes displayed different physical properties (e.g. in droplet growth and adhesion) than those containing inactive ribozymes. Additionally, synthetic, non-NA coacervates have been shown to sequester oligonucleotides and compartmentalize RNA catalysis [99] and to enhance ribozyme activity within the coacervate microenvironment [100, 101]. This suggests the potential for coacervates to modulate and enhance enzymatic reactions, potentially supporting origin of life and protocell theories.

4.4. Controlled droplet formation and dissolution

Biological phase-separated compartments can form or dissolve in response to biochemical cues [82]. Mimicking this, Lee *et al.* designed NAJs that form droplets in response to the addition of sequence-specific single strands that prevent self-binding of NAJ arms [42]. Do *et al.* demonstrated NAJ droplet formation upon the addition of a cross-linking ssDNA strand and droplet dissolution upon the addition of a second competing strand [91]. A related strategy was utilized by Agarwal *et al.* to achieve multiple cycles of droplet dissolution and reformation [102]. A strategy not based on ssDNA strands was introduced by Fabrini *et al.*, who incorporated cation-sensitive G quadruplexes into cholesterol-decorated NAJs, and showed that cation addition/removal led to the appearance/disappearance of NAJ condensates[103].

NA liquid formation and dissolution has also been coupled to enzymatic reactions. For example, Aumiller and Keating [104] and Nakashima *et al.* [105] demonstrated control of NA coacervate formation and dissolution through enzymatic (de)phosphorylation of component peptides. Deng and Walther created NAJ liquids where phase separation is triggered by ligating short DNA segments into extended branched structures, while dissolution is carried out by restriction enzymes that cut the long DNA into short segments (Fig. 8A) [92]. In a study also related to NA cleavage, Sato *et al.* demonstrated a 'driven demixing' behavior, in which a mixed 3-component NAJ droplet separates and forms two orthogonal droplets upon enzymatic cleavage of one of the components (Fig. 8B) [46]; subsequent studies achieved similar effects using photolysis [106] or strand displacement reactions [96].

Saleh *et al.* [107] designed NAJs with recognition sites for a restriction enzyme whose addition thus resulted in droplet dissolution [107]. These authors showed, through quantification of the scaling properties of droplet shrinkage, two distinct physical mechanisms of dissolution in which the enzyme acted either only on the droplet, or throughout its bulk, with the dominant mechanism dependent on the proximity of the system to the phase boundary [107].

A subsequent study of the NAJ/restriction enzyme system [108] showed that droplets that permit enzyme penetration are associated with the formation of vacuoles

that grow, pop, and grow again. Vacuole growth was caused by the osmotic pressure of accumulated restriction fragments, a mechanism the authors confirmed quantitatively. Interestingly, this work showed that vacuole popping could cause locomotion of the NAJ droplet through a jetting effect caused by the osmotic pressure (Fig. 8C), with typical speeds of ≈ 50 nm/s [108].

Recent work by Tayar *et al.* showed that NAJ droplet dissolution can also be driven mechanically, by active stresses [93]. Specifically, the authors coupled NAJ droplets to a motor-driven microtubule network undergoing chaotic active flow, and observed droplets to be dramatically extended and, eventually, to break up (Fig. 8D). Remarkably, fluorescence correlation measurements revealed that high levels of active stress were able to completely dissolve droplets down to single NAJ particles [93]. This mechanical coupling also resulted in changes to the kinetic phase diagram, including a lowered effective critical-point temperature and a narrowed apparent coexistence region.

4.5. Interfacial engineering

Enrichment of solutes at the droplet interface is another powerful technique for modulating NA liquid functionality, particularly as it permits control over the interactions between environments inside and outside NAJ liquids. For example, Nguyen *et al.* discovered the ability to exploit entropic confinement effects so as to target long dsDNAs to an NAJ droplet interface [53] (Fig. 9A). In a following study, Gao *et al.* showed such "long DNA surfactants" can be utilized to tune mean NAJ droplet size, from tens of microns down to tens of nanometers [109]. This was attributed to retardation of coalesence by an inter-droplet disjoining pressure caused by the brush-like layer of long DNA on the droplet interfaces [109], an effect reminiscent of the mechanisms that govern size distributions in dispersion polymerization of monodisperse colloids [110]. Similar size control has been demonstrated in cholesterol-modified systems that use additional NAJs, with only one active sticky-end, as the surfactant [111]. Interfacial engineering has also been achieved using small unilamellar lipid vesicles (SUVs) that adhere to the cholesterol-modified NAJ droplet interface (Fig. 9B). [86].

5. Conclusion

The emerging field of biomolecular phase-separated liquids composed of NAJs has made substantial progress in characterizing the equilibria, dynamics, and materials properties of NAJ liquids. Indeed, precise experimental and theoretical results have characterized the phase diagrams and viscoelastic behaviors of NAJ liquids, including a growing understanding of how these properties vary with the microscopic structure of the phase-separating components. This quantitative physical understanding has permitted researchers to begin to develop functional NAJ liquids that form complex structures and/or are capable of active, responsive behaviors, with the general goals of mimicking life-like processes or creating materials for specific applications.

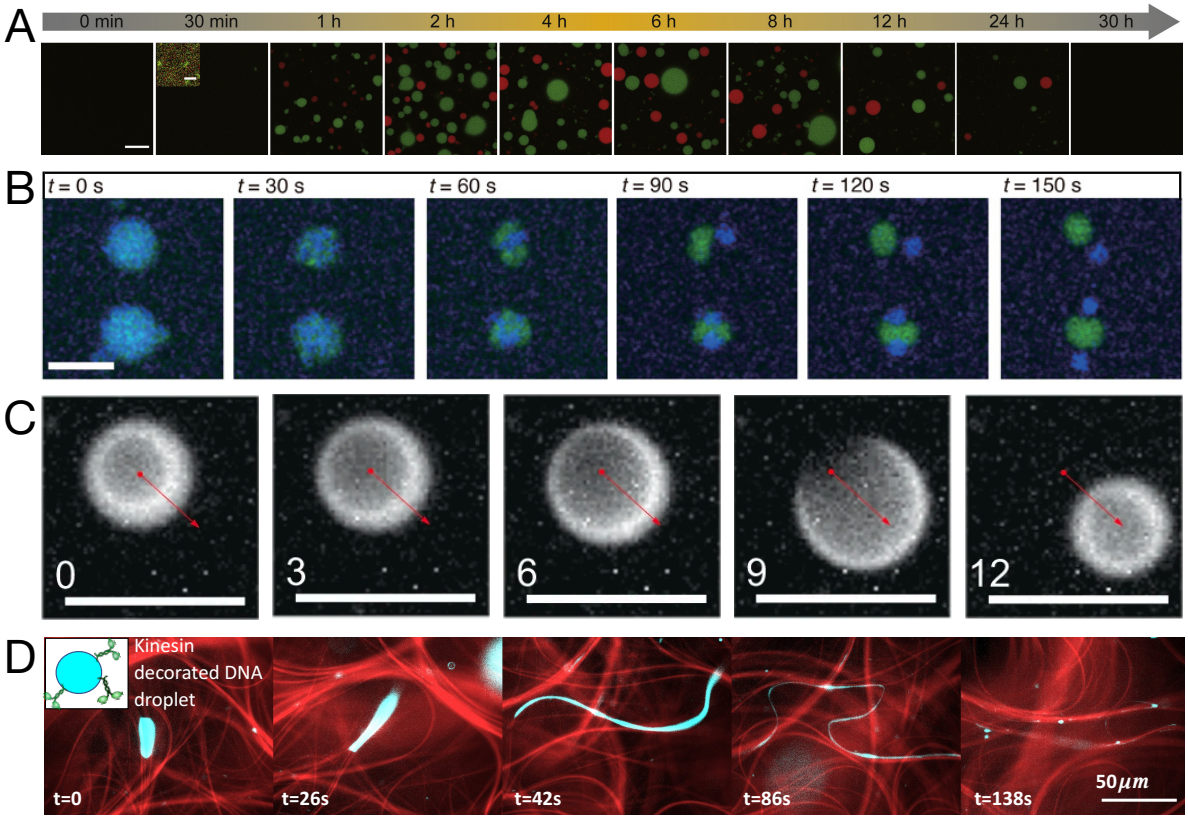

Figure 8. Non-equilibrium NA droplet behaviors. (A) Multiphase DNA coacervate formation and dissolution, enabled by ATP-powered ligation and endonuclease-controlled restriction. Scale bar 20 μm; inset scale bar 4 μm. Reprinted with permission from [92], with permission from Elsevier. (B) NAJ droplet fission as a cross-linker particle is cleaved by RNase A. Scale bar 20 μm. Adapted from [46]. Copyright The Authors, some rights reserved; exclusive licensee AAAS. Distributed under a CC BY-NC 4.0 license. Reprinted with permission from AAAS. Panels excerpted from a larger figure. (C) NAJ droplet motility resulting from vacuole popping. Scale bar 80 μm. Time displayed in minutes. Adapted with permission from [108], excerpted from a larger figure. (D) NAJ droplets mechanically coupled to an active network of microtubule filaments are elongated and ultimately break into daughter droplets. Adapted with permission from [93].

The contrast between NAJ liquids and NA coacervates is instructive. The study of coacervates is much older, and more advanced functional (e.g. biochemical) activities have been embedded into NA coacervates. Yet, a significant advantage of the NAJ liquid is its simplicity, which arises from its dependence on well-characterized DNA hybridization bonds between particles whose structure can be precisely tuned. In contrast, the electrostatic interactions driving coacervate formation defy simple characterization. Thus, despite their relative newness, NAJ liquids are more theoretically tractable, a powerful feature that should enable rapid advances in the field.

Throughout this review, we have noted areas where challenges remain. For example, NAJ interfacial structure is poorly understood, and more work is needed to achieve a

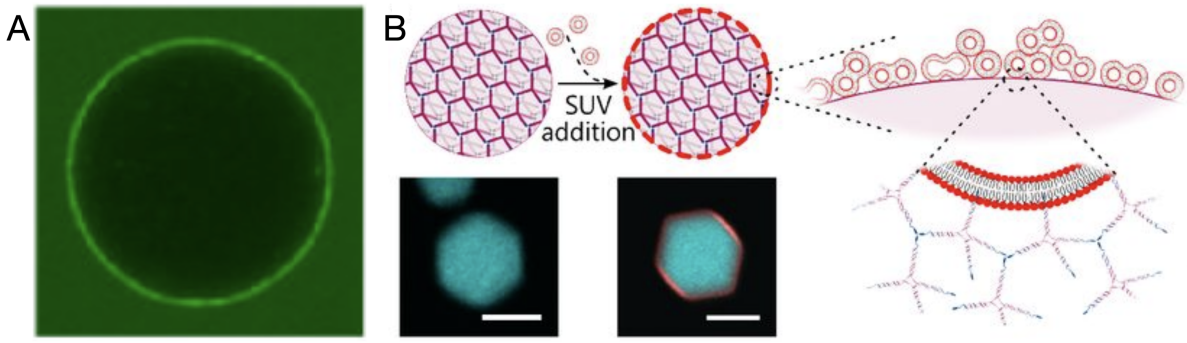

Figure 9. Interfacial engineering of NAJ droplets. (A) dsDNA adhered to an NAJ droplet interface, but excluded from the interior. Droplet is of order 20 μm. Reprinted with permission from [53]. Copyright 2019 American Chemical Society. (B) SUVs adhered to cholesterol-modified NAJ assemblies, forming a shell around them. Scale bars 10 μm. Reprinted with permission from [86], excerpted from a larger figure.

comprehensive understanding of the connection between NAJ liquid microstructure and macroscopic properties. More specific open questions are as follows:

1) There is a fundamental dichotomy between the colloidal understanding of NAJ liquids (e.g. rooted in Wertheim theory), and the polymeric approach to understanding NA coacervates (e.g. relying on Voorn-Overbeek and Flory-Huggins models). This modeling difference is related to a microstructural difference: the ability of constituent particles to entangle, which has generally not been considered for NAJs, but obviously occurs within coacervates. Fundamentally, though, NAJs still have polymeric traits, and certain recent works have indeed suggested that entanglement can play a role [112, 113]. The boundary between colloid-like and entangled behavior is an interesting area of investigation.

2) As detailed throughout, NA liquids can condense via two mechanisms: DNA hybridization or electrostatic attraction with oppositely charged molecules. However, the distinction between these is not so clear cut– for example, even the most simple NAJ liquid relies heavily on electrostatics, as salt is needed to stabilize the sticky-end bonds. Further exploration of the competition and/or cooperation of these two phase-separating mechanisms could help elucidate the complex heterotypic interactions present in biology, as biological condensates can contain many components with multiple possible interactions driving phase separation [82].

3) NA liquids provide a promising avenue to explore active, non-equilibrium behaviors that are analogous to biological liquids. Much of the relevant effort, discussed above, has focused on engineering NA liquids that offer "synthetic cell" functionalities, e.g. in creating compartments and interfacing with biochemical reactions. A notable exciting direction along those lines are recent reports demonstrating the ability to create and control NAJ liquids using transcription reactions [114, 115]; such systems would enable investigation of the interplay of active genetic processes and liquid material behavior. That said, a general critique of much present 'synthetic cell' work is that

it relies on somewhat qualitative and phenomenological demonstrations of functional behaviors. Unlike condensates in living cells, NA liquids are easily modified at the molecular scale, and can be measured to a high degree of precision. This should enable highly quantitative experimental study of NA liquid behaviors which, through comparison to appropriate models, would be powerful in determining underlying physical mechanisms. However, relatively few studies have taken this approach, despite a growing theoretical literature on active-liquid behaviors that has yet to be tested [116, 117, 118, 119]. There is thus a significant opportunity for advancement in this field through hard-nosed experimental physics approaches.

4) Perhaps in part due to the relatively qualitative nature of some of the work in this nascent field, the relevance of many of these systems to applications has not been seriously explored. Indeed, regarding NAJ liquids, we are aware of only a handful of works that even suggest specific applications [109, 91, 96]. As with many areas of NA nanotechnology, we foresee that any applications will need to balance the extraordinary nanoscopic control and functionality offered by NAs with various practical issues, such as chemical stability, robustness, and cost. The revolution in nucleic acid therapeutics[120], as embodied by the mRNA-based COVID vaccines[121], perhaps offers some perspective regarding, on one hand, the enormous potential, and, on the other, the huge practical hurdles that can be present.

Overall, this review has demonstrated that the liquid state of NAs offers a variety of unique and powerful features, and interesting physical questions, though with a range of open questions and future challenges; we look forward to watching the field continue to evolve.

Acknowledgements

This work was partially supported by the W.M. Keck Foundation, by the National Science Foundation under Award No. 2005189, and by the MRSEC Program of the National Science Foundation under Award No. DMR 2308708.

References

[1] Hendrik Gerard Bungenberg de Jong and Hugo R Kruyt. Coacervation (partial miscibility in colloid systems). *Proc. Koninklijke Nederlandse Akademie Wetenschappen*, 32:849–856, 1929.

[2] Wei Wei, Yerpeng Tan, Nadine R Martinez Rodriguez, Jing Yu, Jacob N Israelachvili, and J Herbert Waite. A mussel-derived one component adhesive coacervate. *Acta biomaterialia*, 10(4):1663–1670, 2014.

[3] Yongdae Shin and Clifford P. Brangwynne. Liquid phase condensation in cell physiology and disease. *Science*, 357(6357):eaaf4382, 2017.

[4] Dan Bracha, Mackenzie T. Walls, and Clifford P. Brangwynne. Probing and engineering liquid-phase organelles. *Nature Biotechnology*, 37(12):1435–1445, December 2019.

[5] Oparin Aleksandr Ivanovich. *The Origin of Life*. Macmillan, 1st edition, 1938.

[6] Annemiek D. Slootbeek, Merlijn H.I. van Haren, Iris B.A. Smokers, and Evan Spruijt. Growth, replication and division enable evolution of coacervate protocells. *Chemical Communications*, 58:11183–11200, 9 2022.

[7] Wolfgang Zauner, Manfred Ogris, and Ernst Wagner. Polylysine-based transfection systems utilizing receptor-mediated delivery. *Advanced Drug Delivery Reviews*, 30:97–113, 1998. Non-viral Gene Delivery Systems.

[8] Jasmina Gačanin, Christopher V Synatschke, and Tanja Weil. Biomedical applications of dna-based hydrogels. *Advanced Functional Materials*, 30(4):1906253, 2020.

[9] Khatcher O. Margossian, Marcel U. Brown, Todd Emrick, and Murugappan Muthukumar. Coacervation in polyzwitterion-polyelectrolyte systems and their potential applications for gastrointestinal drug delivery platforms. *Nature Communications*, 13, 12 2022.

[10] Erica Del Grosso, Elisa Franco, Leonard J. Prins, and Francesco Ricci. Dissipative dna nanotechnology. *Nature Chemistry*, 14(6):600–613, 2022.

[11] Alex Hoose, Richard Vellacott, Marko Storch, Paul S. Freemont, and Maxim G. Ryadnov. Dna synthesis technologies to close the gene writing gap. *Nature Reviews Chemistry*, 7:144–161, 3 2023.

[12] Hirotake Udono, Jing Gong, Yusuke Sato, and Masahiro Takinoue. Dna droplets: Intelligent, dynamic fluid. *Advanced Biology*, 7(3):2200180, 2023.

[13] Sam Wilken, Aria Chaderjian, and Omar A. Saleh. Spatial organization of phase-separated dna droplets. *Phys. Rev. X*, 13:031014, Aug 2023.

[14] Paulo L. Onuchic, Anthony N. Milin, Ibraheem Alshareedah, Ashok A. Deniz, and Priya R. Banerjee. Divalent cations can control a switch-like behavior in heterotypic and homotypic rna coacervates. *Scientific Reports*, 9, 12 2019.

[15] Philip C. Bevilacqua, Allison M. Williams, Hong-Li Chou, and Sarah M. Assmann. Rna multimerization as an organizing force for liquid–liquid phase separation. *RNA*, 28(1):16–26, 2022.

[16] Silvia Biffi, Roberto Cerbino, Francesca Bomboi, Elvezia Maria Paraboschi, Rosanna Asselta, Francesco Sciortino, and Tommaso Bellini. Phase behavior and critical activated dynamics of limited-valence dna nanostars. *Proceedings of the National Academy of Sciences*, 110(39):15633–15637, 2013.

[17] B. Alberts and National Center for Biotechnology Information (Estats Units d'Amèrica). *Molecular Biology of the Cell*. Garland, 2004.

[18] David M. J. Lilley. Structures of helical junctions in nucleic acids. *Quarterly Reviews of Biophysics*, 33(2):109–159, 2000.

[19] Soong Ho Um, Jong Bum Lee, Nokyoung Park, Sang Yeon Kwon, Christopher C Umbach, and Dan Luo. Enzyme-catalysed assembly of dna hydrogel. *Nature materials*, 5(10):797–801, 2006.

[20] Paul S Weiss. A conversation with prof. ned seeman: Founder of dna nanotechnology. *ACS Nano*, 2(6):1089–1096, 2008.

[21] Nadrian C Seeman. Nucleic acid junctions and lattices. *Journal of theoretical biology*, 99(2):237–247, 1982.

[22] Nadrian C Seeman and Neville R Kallenbach. Dna branched junctions. *Annual review of biophysics and biomolecular structure*, 23(1):53–86, 1994.

[23] Yu Shao, Chuang Li, Xu Zhou, Ping Chen, Zhongqiang Yang, Zhibo Li, and Dongsheng Liu. Responsive polypeptide-dna hydrogel crosslinked by g-quadruplex. *Acta Chimica Sinica*, 73(8):815, 2015.

[24] Zhiguang Wang, Ruipeng Chen, Shiping Yang, Shuang Li, and Zhixian Gao. Design and application of stimuli-responsive dna hydrogels: A review. *Materials Today Bio*, 16, 12 2022.

[25] Peter H Poole, Francesco Sciortino, Ulrich Essmann, and H Eugene Stanley. Phase behaviour of metastable water. *Nature*, 360(6402):324–328, 1992.

[26] George S Kell. Density, thermal expansivity, and compressibility of liquid water from 0. deg. to 150. deg.. correlations and tables for atmospheric pressure and saturation reviewed and expressed on 1968 temperature scale. *Journal of Chemical and Engineering data*, 20(1):97–105, 1975.

[27] Jeremy C Palmer, Peter H Poole, Francesco Sciortino, and Pablo G Debenedetti. Advances in

computational studies of the liquid–liquid transition in water and water-like models. *Chemical reviews*, 118(18):9129–9151, 2018.

[28] Francesca Bomboi, Silvia Biffi, Roberto Cerbino, Tommaso Bellini, Federico Bordi, and Francesco Sciortino. Equilibrium gels of trivalent dna-nanostars: Effect of the ionic strength on the dynamics. *The European Physical Journal E*, 38:1–8, 2015.

[29] MS Wertheim. Thermodynamic perturbation theory of polymerization. *The Journal of chemical physics*, 87(12):7323–7331, 1987.

[30] Walter G Chapman, Keith E Gubbins, George Jackson, and Maciej Radosz. Saft: Equation-of-state solution model for associating fluids. *Fluid Phase Equilibria*, 52:31–38, 1989.

[31] Carl T Lira, J Richard Elliott, Sumnesh Gupta, and Walter G Chapman. Wertheim's association theory for phase equilibrium modeling in chemical engineering practice. *Industrial & Engineering Chemistry Research*, 61(42):15678–15713, 2022.

[32] Bennett D Marshall, Deepti Ballal, and Walter G Chapman. Wertheim's association theory applied to one site patchy colloids: Beyond the single bonding condition. *The Journal of chemical physics*, 137(10), 2012.

[33] Lorenzo Rovigatti, Francesca Bomboi, and Francesco Sciortino. Accurate phase diagram of tetravalent dna nanostars. *The Journal of Chemical Physics*, 140(15), 2014.

[34] Emanuele Locatelli and Lorenzo Rovigatti. An accurate estimate of the free energy and phase diagram of all-dna bulk fluids. *Polymers*, 10(4):447, 2018.

[35] John SantaLucia Jr and Donald Hicks. The thermodynamics of dna structural motifs. *Annu. Rev. Biophys. Biomol. Struct.*, 33:415–440, 2004.

[36] Emanuela Bianchi, Julio Largo, Piero Tartaglia, Emanuela Zaccarelli, and Francesco Sciortino. Phase diagram of patchy colloids: Towards empty liquids. *Physical review letters*, 97(16):168301, 2006.

[37] Nathaniel Conrad, Grace Chang, Deborah K Fygenson, and Omar A Saleh. Emulsion imaging of a dna nanostar condensate phase diagram reveals valence and electrostatic effects. *The Journal of Chemical Physics*, 157(23), 2022.

[38] Byoung-jin Jeon, Dan T Nguyen, Gabrielle R Abraham, Nathaniel Conrad, Deborah K Fygenson, and Omar A Saleh. Salt-dependent properties of a coacervate-like, self-assembled dna liquid. *Soft Matter*, 14(34):7009–7015, 2018.

[39] Francesco Sciortino and Emanuela Zaccarelli. Equilibrium gels of limited valence colloids. *Current opinion in colloid & interface science*, 30:90–96, 2017.

[40] Paul J Hagerman. Flexibility of dna. *Annual Review of Biophysics and Biophysical Chemistry*, 17:265–286, 1988. PMID: 3293588.

[41] Francesco Spinozzi, Maria Grazia Ortore, Giovanni Nava, Francesca Bomboi, Federica Carducci, Heinz Amenitsch, Tommaso Bellini, Francesco Sciortino, and Paolo Mariani. Gelling without structuring: a saxs study of the interactions among dna nanostars. *Langmuir*, 36(35):10387–10396, 2020.

[42] Taehyun Lee, Sungho Do, Jae Gyung Lee, Do-Nyun Kim, and Yongdae Shin. The flexibility-based modulation of dna nanostar phase separation. *Nanoscale*, 13(41):17638–17647, 2021.

[43] Siddharth Agarwal, Dino Osmanovic, Melissa A Klocke, and Elisa Franco. The growth rate of dna condensate droplets increases with the size of participating subunits. *ACS nano*, 16(8):11842–11851, 2022.

[44] Lorenzo Rovigatti, Frank Smallenburg, Flavio Romano, and Francesco Sciortino. Gels of dna nanostars never crystallize. *ACS nano*, 8(4):3567–3574, 2014.

[45] Dan T Nguyen and Omar A Saleh. Tuning phase and aging of dna hydrogels through molecular design. *Soft Matter*, 13(32):5421–5427, 2017.

[46] Yusuke Sato, Tetsuro Sakamoto, and Masahiro Takinoue. Sequence-based engineering of dynamic functions of micrometer-sized dna droplets. *Science advances*, 6(23):eaba3471, 2020.

[47] Silvia Biffi, Roberto Cerbino, Giovanni Nava, Francesca Bomboi, Francesco Sciortino, and Tommaso Bellini. Equilibrium gels of low-valence dna nanostars: a colloidal model for strong

glass formers. *Soft Matter*, 11(16):3132–3138, 2015.

[48] Javier Fernandez-Castanon, Silvio Bianchi, Filippo Saglimbeni, Roberto Di Leonardo, and Francesco Sciortino. Microrheology of dna hydrogel gelling and melting on cooling. *Soft Matter*, 14(31):6431–6438, 2018.

[49] Nathaniel Conrad, Tynan Kennedy, Deborah K Fygenson, and Omar A Saleh. Increasing valence pushes dna nanostar networks to the isostatic point. *Proceedings of the National Academy of Sciences*, 116(15):7238–7243, 2019.

[50] J Clerk Maxwell. L. on the calculation of the equilibrium and stiffness of frames. *The London, Edinburgh, and Dublin Philosophical Magazine and Journal of Science*, 27(182):294–299, 1864.

[51] Chase P. Broedersz, Xiaoming Mao, Tom C. Lubensky, and Frederick C. MacKintosh. Criticality and isostaticity in fibre networks. *Nat Phys*, 7(12):983–988, 2011.

[52] Robert L. Baldwin. *Weak Interactions in Protein Folding: Hydrophobic Free Energy, van der Waals Interactions, Peptide Hydrogen Bonds, and Peptide Solvation*, pages 127–162. 2005.

[53] Dan T. Nguyen, Byoung-jin Jeon, Gabrielle R. Abraham, and Omar A. Saleh. Length-dependence and spatial structure of dna partitioning into a dna liquid. *Langmuir*, 35(46):14849–14854, 2019. PMID: 31638820.

[54] Yusuke Sato and Masahiro Takinoue. Sequence-dependent fusion dynamics and physical properties of dna droplets. *Nanoscale Advances*, 5(7):1919–1925, 2023.

[55] Evan Spruijt, Joris Sprakel, Martien A Cohen Stuart, and Jasper van der Gucht. Interfacial tension between a complex coacervate phase and its coexisting aqueous phase. *Soft Matter*, 6(1):172–178, 2010.

[56] Clifford P. Brangwynne, Christian R. Eckmann, David S. Courson, Agata Rybarska, Carsten Hoege, Jöbin Gharakhani, Frank Jülicher, and Anthony A. Hyman. Germline p granules are liquid droplets that localize by controlled dissolution/condensation. *Science*, 324(5935):1729–1732, 2009.

[57] Andrea Pelissetto and Ettore Vicari. Critical phenomena and renormalization-group theory. *Physics Reports*, 368(6):549–727, 2002.

[58] A Coniglio and W Klein. Clusters and ising critical droplets: a renormalisation group approach. *Journal of Physics A: Mathematical and General*, 13(8):2775, 1980.

[59] J. T. Overbeek and M. J. Voorn. Phase separation in polyelectrolyte solutions. theory of complex coacervation. *Journal of cellular physiology. Supplement*, 49, 1957.

[60] Paul John Flory. *Principles of Polymer Chemistry*. Cornell University Press, 1953.

[61] Peter Debye and Erich Hückel. Zur theorie der elektrolyte. ii. das grenzgesetz für die elektrische leitfähigkeit. *Physikalische Zeitschrift*, 24(15):305–325, 1923.

[62] Evan Spruijt, Adrie H Westphal, Jan Willem Borst, Martien A Cohen Stuart, and Jasper van der Gucht. Binodal compositions of polyelectrolyte complexes. *Macromolecules*, 43(15):6476–6484, 2010.

[63] Nicola Galvanetto, Miloš T. Ivanović, Aritra Chowdhury, Andrea Sottini, Mark F. Nüesch, Daniel Nettels, Robert B. Best, and Benjamin Schuler. Extreme dynamics in a biomolecular condensate. *Nature*, 7 2023.

[64] Yanxian Lin, James Mccarty, Jennifer N Rauch, Kris T Delaney, Kenneth S Kosik, Glenn H Fredrickson, Joan-Emma Shea, and Songi Han. Narrow equilibrium window for complex coacervation of tau and rna under cellular conditions. *eLife*, 2019.

[65] Kris T. Delaney and Glenn H. Fredrickson. Theory of polyelectrolyte complexation - complex coacervates are self-coacervates. *Journal of Chemical Physics*, 146, 6 2017.

[66] Michael Rubinstein, Qi Liao, and Sergey Panyukov. Structure of liquid coacervates formed by oppositely charged polyelectrolytes. *Macromolecules*, 51:9572–9588, 12 2018.

[67] Ankur Jain and Ronald D Vale. Rna phase transitions in repeat expansion disorders. *Nature*, 546:243–247, 2017.

[68] Rémi Merindol, Sebastian Loescher, Avik Samanta, and Andreas Walther. Pathway-controlled formation of mesostructured all-dna colloids and superstructures. *Nature nanotechnology*,

13(8):730–738, 2018.

[69] Remi Merindol, Giovanne Delechiave, Laura Heinen, Luiz Henrique Catalani, and Andreas Walther. Modular design of programmable mechanofluorescent dna hydrogels. *Nature Communications*, 10(1):528, 2019.

[70] Jong Bum Lee, Songming Peng, Dayong Yang, Young Hoon Roh, Hisakage Funabashi, Nokyoung Park, Edward J Rice, Liwei Chen, Rong Long, Mingming Wu, et al. A mechanical metamaterial made from a dna hydrogel. *Nature nanotechnology*, 7(12):816–820, 2012.

[71] Raghav R. Poudyal, Jacob P. Sieg, Bede Portz, Christine D. Keating, and Philip C. Bevilacqua. Rna sequence and structure control assembly and function of rna condensates. *RNA*, 27(12):1589–1601, 2021.

[72] Gable M Wadsworth, Walter J Zahurancik, Xiangze Zeng, Paul Pullara, Lien B Lai, Vaishnavi Sidharthan, Rohit V Pappu, Venkat Gopalan, and Priya R Banerjee. Rnas undergo phase transitions with lower critical solution temperatures. *bioRxiv*, 2022.

[73] Youri Timsit and Dino Moras. Groove-backbone interaction in b-dna: Implication for dna condensation and recombination. *Journal of Molecular Biology*, 221:919–940, 1991.

[74] Juan Pelta, Françoise Livolant, and Jean Louis Sikorav. Dna aggregation induced by polyamines and cobalthexamine. *Journal of Biological Chemistry*, 271:5656–5662, 3 1996.

[75] Michi Nakata, Giuliano Zanchetta, Brandon D Chapman, Christopher D Jones, Julie O Cross, Ronald Pindak, Tommaso Bellini, and Noel A Clark. End-to-end stacking and liquid crystal condensation of 6– to 20–base pair dna duplexes. *Science*, 318:1276–1279, 2007.

[76] Anisha Shakya and John T. King. Dna local-flexibility-dependent assembly of phase-separated liquid droplets. *Biophysical Journal*, 115:1840–1847, 2018.

[77] Tommaso P Fraccia and Tony Z Jia. Liquid crystal coacervates composed of short double-stranded dna and cationic peptides. *ACS Nano*, 14:15071–15082, 11 2020.

[78] Lars Onsager. The effects of shape on the interaction of colloidal particles. *Annals of the New York Academy of Sciences*, 51(4):627–659, 1949.

[79] M M Daly and A E Mirsky. Histones with high lysine content. *The Journal of General Physiology*, 38:405, 1955.

[80] Donald E Olins. Interaction of lysine-rich histones and dna. *J. Mol. Biol*, 43:439–460, 1969.

[81] Jeffrey R. Vieregg, Michael Lueckheide, Amanda B. Marciel, Lorraine Leon, Alex J. Bologna, Josean Reyes Rivera, and Matthew V. Tirrell. Oligonucleotide-peptide complexes: Phase control by hybridization. *Journal of the American Chemical Society*, 140:1632–1638, 2 2018.

[82] Salman F Banani, Hyun O Lee, Anthony A Hyman, and Michael K Rosen. Biomolecular condensates: organizers of cellular biochemistry. *Nature reviews Molecular cell biology*, 18(5):285–298, 2017.

[83] Marina Feric, Nilesh Vaidya, Tyler S. Harmon, Diana M. Mitrea, Lian Zhu, Tiffany M. Richardson, Richard W. Kriwacki, Rohit V. Pappu, and Clifford P. Brangwynne. Coexisting liquid phases underlie nucleolar subcompartments. *Cell*, 165:1686–1697, 6 2016.

[84] Byoung-jin Jeon, Dan T. Nguyen, and Omar A. Saleh. Sequence-controlled adhesion and microemulsification in a two-phase system of dna liquid droplets. *The Journal of Physical Chemistry B*, 124(40):8888–8895, 2020.

[85] Rachel S. Fisher and Shana Elbaum-Garfinkle. Tunable multiphase dynamics of arginine and lysine liquid condensates. *Nature Communications*, 11:1–10, 12 2020.

[86] Layla Malouf, Diana A Tanase, Giacomo Fabrini, Miguel Paez-Perez, Adrian Leathers, Michael J Booth, and Lorenzo Di Michele. Sculpting dna-based synthetic cells through phase separation and phase-targeted activity. *bioRxiv*, 2023.

[87] Sheng Mao, Milena S Chakraverti-Wuerthwein, Hunter Gaudio, and Andrej Košmrlj. Designing the morphology of separated phases in multicomponent liquid mixtures. *Physical review letters*, 125(21):218003, 2020.

[88] Tiemei Lu and Evan Spruijt. Multiphase complex coacervate droplets. *Journal of the American Chemical Society*, 142:2905–2914, 2 2020.

[89] Taranpreet Kaur, Muralikrishna Raju, Ibraheem Alshareedah, Richoo B. Davis, Davit A. Potoyan, and Priya R. Banerjee. Sequence-encoded and composition-dependent protein-rna interactions control multiphasic condensate morphologies. *Nature Communications 2021 12:1*, 12:1–16, 2 2021.

[90] Saehyun Choi, McCauley C.O. Meyer, Philip C. Bevilacqua, and Christine D. Keating. Phase-specific rna accumulation and duplex thermodynamics in multiphase coacervate models for membraneless organelles. *Nature Chemistry 2022 14:10*, 14:1110–1117, 6 2022.

[91] Sungho Do, Chanseok Lee, Taehyun Lee, Do-Nyun Kim, and Yongdae Shin. Engineering dna-based synthetic condensates with programmable material properties, compositions, and functionalities. *Science Advances*, 8(41):eabj1771, 2022.

[92] Jie Deng and Andreas Walther. Programmable atp-fueled dna coacervates by transient liquid-liquid phase separation. *Chem*, 6(12):3329–3343, 2020.

[93] Alexandra M. Tayar, Fernando Caballero, Trevor Anderberg, Omar A. Saleh, M. Cristina Marchetti, and Zvonimir Dogic. Controlling liquid–liquid phase behaviour with an active fluid. *Nature Materials*, 2023.

[94] Adrian Leathers, Michal Walczak, Ryan A. Brady, Assala Al Samad, Jurij Kotar, Michael J. Booth, Pietro Cicuta, and Lorenzo Di Michele. Reaction–diffusion patterning of dna-based artificial cells. *Journal of the American Chemical Society*, 144(38):17468–17476, 2022.

[95] Simon Alberti, Amy Gladfelter, and Tanja Mittag. Considerations and challenges in studying liquid-liquid phase separation and biomolecular condensates. *Cell*, 176(3):419–434, 2019.

[96] Jing Gong, Nozomi Tsumura, Yusuke Sato, and Masahiro Takinoue. Computational dna droplets recognizing mirna sequence inputs based on liquid–liquid phase separation. *Advanced Functional Materials*, 32(37):2202322, 2022.

[97] Ludo L. J. Schoenmakers, N. Amy Yewdall, Tiemei Lu, Alain A. M. André, Frank. H.T. Nelissen, Evan Spruijt, and Wilhelm T. S. Huck. In vitro transcription–translation in an artificial biomolecular condensate. *ACS Synthetic Biology*, 7 2023.

[98] Kristian Kyle Le Vay, Elia Salibi, Basusree Ghosh, T Y Dora Tang, and Hannes Mutschler. Ribozyme activity modulates the physical properties of rna–peptide coacervates. *eLife*, 12:e83543, 6 2023.

[99] Björn Drobot, Juan M. Iglesias-Artola, Kristian Le Vay, Viktoria Mayr, Mrityunjoy Kar, Moritz Kreysing, Hannes Mutschler, and T. Y.Dora Tang. Compartmentalised rna catalysis in membrane-free coacervate protocells. *Nature Communications*, 9, 12 2018.

[100] Raghav R. Poudyal, Rebecca M. Guth-Metzler, Andrew J. Veenis, Erica A. Frankel, Christine D. Keating, and Philip C. Bevilacqua. Template-directed rna polymerization and enhanced ribozyme catalysis inside membraneless compartments formed by coacervates. *Nature Communications*, 10:1–13, 12 2019.

[101] Raghav R. Poudyal, Christine D. Keating, and Philip C. Bevilacqua. Polyanion-assisted ribozyme catalysis inside complex coacervates. *ACS Chemical Biology*, 14:1243–1248, 6 2019.

[102] Siddharth Agarwal, Dino Osmanovic, Melissa Klocke, and Elisa Franco. Biochemical control of dna condensation. *Research Square*, 2022.

[103] Giacomo Fabrini, Aisling Minard, Ryan A. Brady, Marco Di Antonio, and Lorenzo Di Michele. Cation-responsive and photocleavable hydrogels from noncanonical amphiphilic dna nanostructures. *Nano Letters*, 22(2):602–611, 2022.

[104] William M Aumiller Jr and Christine D Keating. Phosphorylation-mediated rna/peptide complex coacervation as a model for intracellular liquid organelles. *Nature chemistry*, 8(2):129–137, 2016.

[105] Karina K Nakashima, Jochem F Baaij, and Evan Spruijt. Reversible generation of coacervate droplets in an enzymatic network. *Soft Matter*, 14:361, 2018.

[106] Mai P. Tran, Rakesh Chatterjee, Yannik Dreher, Julius Fichtler, Kevin Jahnke, Lennart Hilbert, Vasily Zaburdaev, and Kerstin Göpfrich. A dna segregation module for synthetic cells. *Small*, 19(13):2202711, 2023.

[107] Omar A. Saleh, Byoung-jin Jeon, and Tim Liedl. Enzymatic degradation of liquid droplets of dna is modulated near the phase boundary. *Proceedings of the National Academy of Sciences*, 117(28):16160–16166, 2020.

[108] Omar A. Saleh, Sam Wilken, Todd M. Squires, and Tim Liedl. Vacuole dynamics and popping-based motility in liquid droplets of dna. *Nature Communications*, 14(1):3574, 2023.

[109] Daqian Gao, Sam Wilken, Anna Nguyen, Gabrielle R. Abraham, Tim Liedl, and Omar A. Saleh. Controlling the size and adhesion of dna droplets using surface-active dna molecules, 2023.

[110] Seth Beck and Ravin Narain. Chapter 3 - polymer synthesis. In *Polymer Science and Nanotechnology*, pages 21–85. Elsevier, 2020.

[111] Michal Walczak, Ryan A. Brady, Leonardo Mancini, Claudia Contini, Roger Rubio-Sánchez, William T. Kaufhold, Pietro Cicuta, and Lorenzo Di Michele. Responsive core-shell dna particles trigger lipid-membrane disruption and bacteria entrapment. *Nature Communications*, 12(1):4743, August 2021.

[112] Giorgia Palombo, Simon Weir, Davide Michieletto, and Yair Augusto Gutierrez Fosado. Topological elasticity in physical gels with limited valence, 2023.

[113] Enrico Lattuada, Tommaso Pietrangeli, and Francesco Sciortino. Interpenetrating gels in binary suspensions of dna nanostars. *The Journal of Chemical Physics*, 157(13), 2022.

[114] Giacomo Fabrini, Sabrina Pia Nuccio, Jaimie Marie Stewart, Shiyi Lin, Anli Tang, Paul W. K. Rothemund, Elisa Franco, Marco Di Antonio, and Lorenzo Di Michele. Co-transcriptional production of programmable rna condensates and synthetic organelles. *bioRxiv*, 2023.

[115] Jaimie Marie Stewart, Shiyi Li, Anli Tang, Melissa Ann Klocke Ann Klocke, Martin Vincent Gobry, Giacomo Fabrini, Lorenzo Di Michele, Paul W.K. Rothemund, and Elisa Franco. Modular rna motifs for orthogonal phase separated compartments. *bioRxiv*, 2023.

[116] David Zwicker, Rabea Seyboldt, Christoph A. Weber, Anthony A. Hyman, and Frank Jülicher. Growth and division of active droplets provides a model for protocells. *Nature Physics*, 13(4):408–413, 2017.

[117] G. Fausti, E. Tjhung, M. E. Cates, and C. Nardini. Capillary interfacial tension in active phase separation. *Phys. Rev. Lett.*, 127:068001, Aug 2021.

[118] Leonardo Demarchi, Andriy Goychuk, Ivan Maryshev, and Erwin Frey. Enzyme-enriched condensates show self-propulsion, positioning, and coexistence. *Phys. Rev. Lett.*, 130:128401, Mar 2023.

[119] Jan Kirschbaum and David Zwicker. Controlling biomolecular condensates via chemical reactions. *Journal of The Royal Society Interface*, 18(179):20210255, 2021.

[120] Jayesh A. Kulkarni, Dominik Witzigmann, Sarah B. Thomson, Sam Chen, Blair R. Leavitt, Pieter R. Cullis, and Roy van der Meel. The current landscape of nucleic acid therapeutics. *Nature Nanotechnology*, 16(6):630–643, 2021.

[121] Xucheng Hou, Tal Zaks, Robert Langer, and Yizhou Dong. Lipid nanoparticles for mrna delivery. *Nature Reviews Materials*, 6(12):1078–1094, 2021.